Trull, J. [et al.] (2018) Controllable coherent backscattering of light in disordered media filled with liquid crystal. *Optics letters*. Vol. 43, Issue 10, pp. 2300-2303. Doi: http://dx.doi.org/10.1364/OL.43.002300.

Trull, J. [et al.] (2018) Controllable coherent backscattering of light in disordered media filled with liquid crystal. *Optics letters*. Vol. 43, Issue 10, pp. 2300-2303. Doi: http://dx.doi.org/10.1364/OL.43.002300.

Controllable coherent backscattering of light in disordered media filled with liquid crystal

JOSÉ TRULL,[1] MARC CUEVAS,[1,2] JOSEP SALUD,[2] CRINA COJOCARU,[1] DAVID O. LÓPEZ[2,*]

[1]Grup de Dinàmica no Linial, Òptica no Linial i Lasers (DONLL), Departament de Física, E.S.E.I.A.A.T. Universitat Politècnica de Catalunya, Colom 11, E-08222 Terrassa, Spain

[2]Grup de Propietas Físiques dels Materials (GRPFM), Departament de Física, E.T.S.E.I.B. Universitat Politècnica de Catalunya, Diagonal 647, E- 08028 Barcelona, Spain

*Corresponding author: david.orencio.lopez@upc.edu

Received XX Month XXXX; revised XX Month, XXXX; accepted XX Month XXXX; posted XX Month XXXX (Doc. ID XXXXX); published XX Month XXXX

We have investigated multiple scattering of light in a disordered system based on liquid crystals for a temperature-controllable random laser. Coherent backscattering measurements at several temperatures have been well fitted by the theoretical model deduced for a random collection of spherical point scatters based on a diffusion approximation. The transport mean free path exclusively depends upon the diffusivity of the liquid crystalline phase of the hybrid scattering system. It is shown how the laser threshold excitation intensity is strongly correlated with the transport mean free path.

OCIS codes: *(290.1350) Backscattering or (280.1350) Backscattering; (160.3710) Liquid crystals; (030.1670) Coherent optical Effects; (140.3460) Lasers; (160.2710) Inhomogeneous optical media; (290.1990) Diffusion*

http://dx.doi.org/10.1364/OL.99.099999

Random photonic materials are structures with a high refractive index contrast in which multiple scattering of light occurs. Light scattering experiments in these materials have been the focus of attention thanks to their promising applications based on light localization properties (weak or strong) that have been realized for instance in the form of random lasers [1-5]. Temperature control of lasing emission in disordered systems based on liquid crystals was proposed in the early 21st century [6,7] but very few attempts of optimization have so far been undertaken [8].

Propagation of light in disordered dielectric materials depends on the scattering strength of the media which can be easily quantified by means of the disorder parameter $k\ell$ [9], where k is the wave vector of light in vacuum and ℓ is the transport mean free path, defined as the average distance traveled by a light ray before the direction of propagation is randomized. Several regimes of propagation may be identified according to the disorder parameter. Anderson or strong localization of light is expected for $k\ell \leq 1$, while propagation is assumed to be described by a diffusive process for $k\ell >1$ (weak localization). The disorder parameter or transport mean free path, ℓ, may be determined by combining predictions of diffusion theory with light scattered by the sample. Several strategies have been followed, depending on the disordered sample: on one hand, total light transmission experiments [10], by measuring the spatial intensity distribution of laterally leaking light [11-13]. On the other hand, the coherent backscattering of light is probably the most used experimental strategy. The first experimental studies on backscattering were carried out in disordered media composed of spherically shaped scatterers[14-16], and were extended to other media like porous glasses [17].

The coherent backscattering of light is an effect where the intensity of the light reflected by a diffusive disordered medium exhibits an angular dependence consequence of phase coherence effects in the constructive interferences of multiple scattering processes. This appears as a peak with a "conic" shape superimposed to the incoherent reflected intensity. The maximum intensity of the peak coincides with the exact direction of backscattering, and the coherent backscattered intensity diminishes away from that direction. The height of the cone is predicted to be twice the incoherent reflected intensity in the exact backscattering direction for circularly polarized light in the helicity preserving channel [18]. The angular width of the cone in which the coherent effects are observed is of the order of the inverse of the disorder parameter $(k\ell)^{-1}$. It should be noted that the incoherent reflected intensity is almost independent of the angle between the incident light and the direction of the outgoing wave [18].

In this paper we present the first experimental measurements of coherent backscattering of a disordered system consisting of a porous borosilicate glass matrix

infiltrated with a liquid crystal and laser dye at several temperatures.

The sample used in our backscattering experiments consists of a disk-shaped, porous disordered matrix made of colorless borosilicate glass powder of arbitrary shape and size ranging from 1 to 10 µm pressed under 0.7 GPa. The disk-shaped structure has about 1 cm diameter and is about 5 mm thick with irregular, truncated and interconnected channels, as is shown in the SEM images of Figure 1 (top side in *xy* plane and lateral side in *yz* plane). The porosity of the glass matrix is estimated to be about 40 % and was infiltrated with a binary mixture of calamitic liquid crystal *n*-(4-*n*-butyloxybenzylidene)-4'-*n'*-octyloaniline (C_4H_9-O-C_6H_4-NCH-C_6H_4-C_8H_{17},hereafter referred as 4O.8) and a small amount of organic dye 4-dicyanometylene-2-methyl-6-p-dimethylamino-stryl-4*H*-pyran (hereafter denoted as DCM). The resulting weight fraction (X) of the DCM in the mixture was 1.20×10^{-3}. The estimated filling rate was of about 40 % of the available porous cavity in a way that we have a hybrid porous disordered system formed by about 60 % of borosilicate glass, about 16 % of liquid crystal, about 0.1 % of laser dye and about 24 % of air. Details of preparation procedure and temperature behavior of the sample are described in [8]. The sample reproduces the different mesogenic phase transitions of the bulk liquid crystal with small shifts of transition temperatures. Three representative temperatures were considered for backscattering experiments, each one related to one of the three liquid crystalline mesophases: 313 K for the sample in the smectic B (SmB) phase, 325 K for the smectic A (SmA) phase and 337 K for the nematic (N) phase.

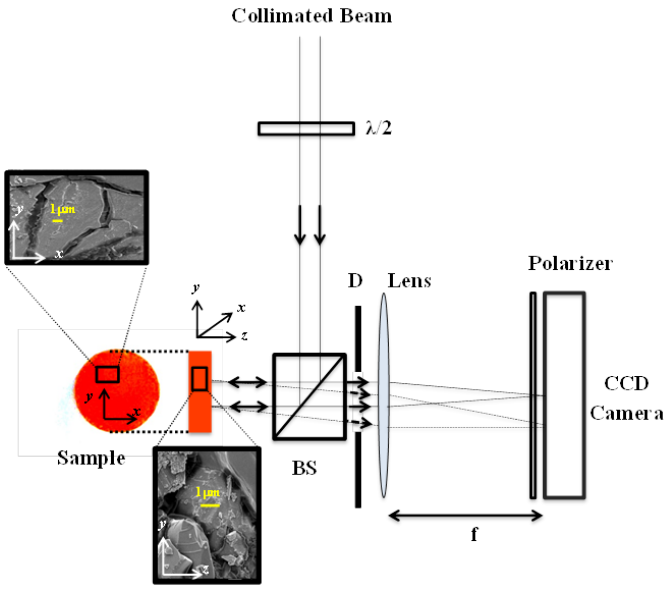

Fig 1. Schematic setup for coherent backscattering experiments. BS and D stand for a non-polarized beam splitter and a diaphragm, respectively. SEM images of the sample at the disk-surface (*xy* plane) and lateral-surface (*zy* plane).

Figure 1 shows the schematic setup used for backscattering measurements. A highly collimated beam at 532 nm from a CW laser source with linear s-polarization (electric field oriented in vertical direction) was incident on the sample after being reflected by a non-polarized cube beam splitter, with a diameter slightly smaller than the sample size. The light scattered form the sample around the backscattering direction was transmitted through the beam splitter, and the s-polarized component was focused using a lens of 200 mm focal length, f, on a charge-coupled device (CCD) camera. The angular resolution in the collected backscattered intensity was of 0.04 mrad. The sample was held on a modified hot stage (TMSG-600), with a temperature controller (TMS-93) (both from linkam) and it was provided with rotational motion around the *z* axis, normal to the sample surface, to obtain an averaged distribution of the backscattered speckle pattern.

Figure 2(a) shows the typical backscattered speckle pattern recorded by the CCD camera for the sample without rotation, at 313 K (SmB phase). The inset of Figure 2a shows the same backscattered pattern with the sample rotating with respect to the *z* axis normal to the sample surface. When the sample rotates, the CCD camera records the averaging over the disordered medium in a way that coherent effects of the backscattering are enhanced. This procedure is needed to obtain the coherent backscattering cone in solid samples and the most efficient average seems to be obtained when the sample rotates with a small precessional motion [18,19].

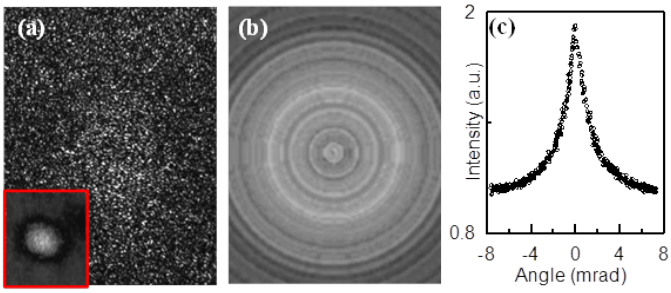

Fig. 2. (a) Speckle pattern obtained by multiple scattering of light in a disordered sample made from borosilicate glass, liquid crystal and organic dye, recorded by a CCD camera at 313 K. The inset shows the multiple scattering of light with the same sample rotating over a *z* axis nearly parallel to the incident light. (b) Pattern obtained by averaging the backscattered intensity over the disordered medium at 313 K. (c) The resulting curve of the angular dependence of the average backscattered intensity.

Figure 2(b) shows the speckle pattern after performing a numerical average of an ensemble of different realizations of the disordered medium. The angular isotropy of the backscattering cone is clearly observed. This means that the sample, a hybrid disordered structure based on liquid crystal, does not seem to show transport mean free path anisotropy, at less within our experimental resolution.

Figure 2(c) shows the resulting average backscattered intensity at 313 K, as a function of the scattering angle with respect to the exact backscattering direction. The intensity values are normalized in regard to the incoherent reflected intensity. The shape of the backscattering cone depends upon the disordered structure at large depths into the sample because the contribution of the scattering long paths is maximum at the exact backscattering direction. Light absorption reduces such scattering long paths in a way that the top of the peak appears rounded [18,19]. In our case, light absorption effect is only due to the DCM dye, and the extremely low amount used minimizes such undesirable effect, as

may be observed in Figure 2(c). The sample thickness is an important parameter to consider in order to minimize finite size effects. According to van der Mark et al. [20], sample thickness of the order of or larger than 32 transport mean free paths are adequate for such experiments.

The procedure to obtain the coherent backscattering cone at several temperatures is the same as illustrated in Figure 2. In a comparative way, Figure 3 shows the coherent backscattering cone for the same sample at three different temperatures, each one representative of the three liquid crystalline phases: SmB at 313 K (empty circles), SmA at 325 K (filled circles) and N at 337 K (empty squares). One may clearly discern that the backscattering cone becomes narrower when the liquid crystalline phases change from SmB to N. The right inset of Figure 3 compares the backscattering cones obtained at two temperatures (filled squares at room temperature and empty circles at 313 K) with the sample in the same SmB phase. Data at room temperature correspond to the sample in the supercooled SmB phase published in [8]. The backscattering cone is insensitive to temperature changes when the liquid crystalline phase remains unchanged. Thus, the observed narrowing of the backscattering cones in Figure 3 is exclusively due to liquid crystalline phase changes, and the chosen temperatures are representative of the disordered system in each liquid crystalline phase.

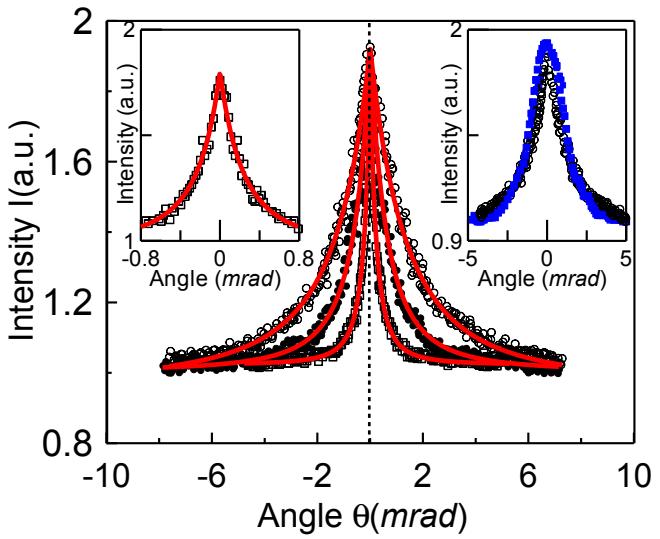

Fig. 3. Average backscattering intensity I as a function of the angle from the exact backscattering direction (θ), for the hybrid sample at three temperatures (o-313 K; •-325 K and □-337 K). The lines correspond to the theoretical model from eq. (1) with eq. (4). The right inset shows a comparison of the backscattering intensity at two temperatures (filled squares at 298 K and empty circles at 313 K) for the sample in the SmB liquid crystalline phase. The left inset shows the detail of the measurements for 337 K together with the theoretical model from eq. (1) with eq.(2).

The normalized backscattered intensity ($I(\theta,\ell)$) data as a function of the scattering angle θ of Figure 3 were fitted to the approximate expression [18-21]:

$$I(\theta,\ell) = \frac{A\gamma_C(\theta,\ell) + \gamma_I(\theta)}{\gamma_I(\theta=0)}. \quad \textbf{(1)}$$

where $\gamma_C(\theta,\ell)$ and $\gamma_I(\theta)$ are the bistatic coefficients for coherent and incoherent scattering, and A is a renormalization factor related to the backscattered intensity enhancement. The incoherent part $\gamma_I(\theta)$ in the angular experimental range is assumed to be almost independent of the angle, and it is verified that $\gamma_C(\theta=0,\ell) = \gamma_I(\theta=0)$. The coherent part $\gamma_C(\theta,\ell)$ responsible for the backscattering cone assuming no surface reflectivity [18,20] is:

$$\gamma_C(\theta,\ell) = \frac{1}{(1+2z_0)(1+u)^2}\left[1 + \frac{1-\exp(-2z_0u)}{u}\right]. \quad \textbf{(2)}$$

where z_0 is assumed to be 0.7104 [20] and $u = k\ell|\sin\theta|$ where $k\ell$ is the disorder parameter obtained from the fitting procedure of experimental data of Figure 3, as listed in Table 1.

Backscattering curves of Figure 3 seem to be well described by eq. (1) with eq. (2), as one may observe in the left-inset of Figure 3 in which the backscattering data and fitting function corresponding to the narrowest peak are shown in an enlarged scale with the classical triangular cusp. However, it should be stressed that eq. (2) is deduced for a random collection of spherical point scatters based on a diffusion approximation for samples in a thick slab geometry. The sample investigated here is far from a collection of point scatters and, in fact, it is closer to a porous glass. Backscattering cones for porous glasses could be affected by the fractal geometry of the surface structure in a way that the cone-shape is different from that obtained from eq. (2) [22].

Table 1. Disorder parameter ($k\ell$), the transport mean free path (ℓ) and the average reflectivity (R) of the sample surface for the representative temperatures of the different liquid crystalline phases.

	SmB (313 K)	SmA (325 K)	N (337 K)
$k\ell$ [a]	294	653	1778
ℓ (μm)[b]	25	55	138
$k\ell$ [c]	330	590	1547
ℓ (μm)[b]	28	50	131
$k\ell$ [d]	208	459	1312
ℓ (μm)[b]	18	39	111
R[d]	0.59	0.47	0.46

[a]Values obtained from fitting procedure according to eq. (1) and eq. (2). [b]Values calculated from $k\ell$ taking into account the wavelength of 532 nm. [c]Values obtained from eq. (3). [d]Values obtained from fitting procedure according to eq. (1) and eq. (4).

Van der Mark et al. [20] established, for practical calculations on thick enough samples (about to or more than 32 transport mean free paths) and parallel polarized incident light, that the full width half-maximum (W) of the "cone" is related to the disorder parameter as:

$$W \approx \frac{0.7\lambda}{2\pi\ell} = \frac{0.7}{k\ell} \quad \textbf{(3)}$$

Results of $k\ell$ from eq. (3) are also listed in Table 1 for comparison. The surface reflection effect reduces the width of the backscattering intensity "cone" in a way that the full width half-maximum (W) must be corrected by a narrowing factor that takes into account the reflectivity of the sample-air interface and the effective refractive index of the sample [23,24]. Lagendijk et al. [23] proposed a relationship for the coherent part $\gamma_C(\theta,\ell)$ introducing a correction for surface reflectivity by means of the parameter ε:

$$\gamma_C(\theta,\ell) = \frac{1}{(1+2(z_0+\varepsilon)(1+u)^2}\left[1+\frac{1+(u\varepsilon-1)exp(-2z_0u)}{u(u\varepsilon+1)}\right] \quad \textbf{(4)}$$

The parameter ε accounts for the correction of the surface reflectivity expressed as R/(1-R); R is the average reflectivity of the sample surface. Eq. (4) combined with eq. (1) allows us to obtain the corrected $k\ell$ parameter by fitting the experimental data of Figure 3. These results together with the R-factors are listed in Table 1.

Figure 4 shows the energy threshold for random laser action of the investigated sample taken from [8] as a function of the surface-reflectivity corrected transport mean free path ℓ read from Table 1. With the purpose of comparison to other closely related scattering system for random laser action, energy threshold and transport mean free path corresponding to a percolated SK11 glass with 7CB liquid crytal+DCM mixture in the nematic phase is included (red symbol). The data was taken from [7]. It is clear how the energy threshold for random laser action in hybrid systems based on liquid crystals is straightforwardly proportional to the transport mean free path of the scattering system which, in turns, exclusively depends on the liquid crystalline phase.

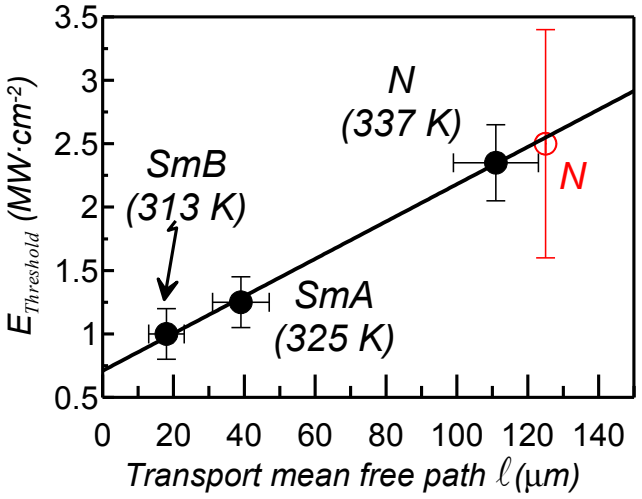

Figure 4- Laser threshold excitation intensity as a function of the transport mean free path for the hybrid sample made from borosilicate glass, liquid crystal and dye (filled circles). Also included is the symbol (empty circle) corresponding to a closely related system in [7].

In conclusion, the transport mean free path of the disordered system formed by a porous borosilicate glass infiltrated with a liquid crystal and laser dye is observed to change with temperature exclusively due to the liquid crystalline phase behavior. Experimental coherent backscattering cone shapes are well described by the theoretical approach of a random collection of spherical point scatters based on a diffusion approximation embodied by the combination of eqs. (1) and (2). The disorder parameter and the transport mean free path calculated by eq. (3) agree with those obtained by the fitting procedure. Table 1 provides an overall comparison of such data. In contrast, the correction of the backscattering cones due to the surface reflectivity of the sample is well addressed by means of eq. (4). The corrected values for the disorder parameter or the transport mean free path are also listed in Table 1.

Finally, Figure 4 shows how the laser energy threshold for this disordered hybrid system based on liquid crystals is strongly driven by the transport mean free path which is exclusively liquid crystalline phase dependent.

Funding. MINECO-FEDER projects: MAT2015-66208-C3-2-P; FIS2015-65998-C2-1-P

References

1. N.M. Lawandy, R.M. Balanchandran, A.S.L. Gomes and E. Sauvain, Nature **368,** 436 (1994).
2. D.S. Wiersma, M.P. van Albada and A. Lagendijk, Nature **373**, 203 (1995).
3. H. Cao, Y.G. Zhao, S.T. Ho, E.W. Seelig, Q.H. Wang and R.P.H. Chang, Phys.Rev.Lett. **82**, 2278 (1999).
4. D.S. Wiersma, Nature Phys. **4**, 359 (2008).
5. D.S. Wiersma, Nature Phys. **539**, 360 (2016).
6. D.S. Wiersma and S. Cavalieri, Nature **414**, 708 (2001).
7. D.S. Wiersma and S. Cavalieri, Phys.Rev.E **66**, 056612 (2002).
8. J. Trull, J. Salud, S. Diez-Berart and D.O. López, Phys.Rev.E **95**, 052704 (2017).
9. D.S. Wiersma, P. Bartolini, A. Lagendijk and R. Righini, Nature **390**, 671 (1997).
10. N. Garcia, A.Z. Genack and A. Lisyansky, Phys.Rev.B **46**, 14475 (1992).
11. J. Taniguchi, H. Murata and Y. Okamura, Appl.Opt. **46**, 2649 (2007).
12. P.M. Johnson, S. Faez and A. Lagendijk, Opt. Exp. **16**, 7435 (2008).
13. M. Leonetti, C. López, Opt. Lett. **36**, 2824 (2011).
14. L. Tsang and A. Ishimaru, J. Opt. Soc. Chem. A **1**, 836 (1984).
15. M.P. van Albada and A. Lagendijk, Phys.Rev.Lett. **55**, 2692 (1985)
16. P.E. Wolf and G. Maret, Phys.Rev.Lett. **55**, 2696 (1985).
17. S. Kawato, T. Hattori, T. Takemori and H. Nakatsuka, Phys.Rev.B **49**, 90 (1994).
18. E. Akkermans, G. Montambaux, *Mesoscopic Physics of Electrons and Photons*, (Cambridge University Press , 2007).
19. D.S. Wiersma, M. P. van Albada and A. Lagendijk, Rev.Sci.Instrum. **66**, 5473 (1995).
20. M.B. van der Mark, M. P. van Albada and A. Lagendijk, Phys.Rev.B **37**, 3575 (1988).
21. D.S. Wiersma, M. P. van Albada, B.A. van Tiggelen and A. Lagendijk, Phys.Rev.Lett. **74**, 4193 (1995).
22. E. Akkermans, P.E. Wolf, R. Maynard and G. Maret, J. Phys. (Paris) **49**, 77 (1988).
23. A. Lagendijk, R. Vreeker and P. DeVries, Phys.Lett.A **136**, 81 (1989).
24. J.X. Zhu, D.J. Pine and D.A. Weitz, Phys.Rev.A **44**, 3948 (1991).